

TOLLMIEIN-SCHLICHTING ROUTE TO ELASTOINERTIAL TURBULENCE

Ashwin Shekar

Department of Chemical and Biological Engineering
University of Wisconsin-Madison
Madison, WI 53706 USA
shekar2@wisc.edu

Richard J. Hommel

Department of Chemical and Biological Engineering
University of Wisconsin-Madison
Madison, WI 53706 USA
hommel@wisc.edu

Ryan M. McMullen

Graduate Aerospace Laboratories
Caltech
Pasadena, CA 91125 USA
mcmullen@caltech.edu

Beverley J. McKeon

Graduate Aerospace Laboratories
Caltech
Pasadena, CA 91125 USA
mckeon@caltech.edu

Michael D. Graham

Department of Chemical and Biological Engineering
University of Wisconsin-Madison
Madison, WI 53706 USA
mdgraham@wisc.edu

ABSTRACT

The so-called elastoinertial regime of turbulence in polymer solutions is dominated by nearly two-dimensional structure. Direct simulations of two-dimensional channel flow of a viscoelastic fluid have revealed the existence of a family of Tollmien-Schlichting (TS) attractors that is nonlinearly self-sustained by viscoelasticity. Here, we describe the evolution of this branch in parameter space and its connections to the Newtonian TS wave and to elastoinertial turbulence (EIT). At Reynolds number $Re=3000$, there is a solution branch with TS-wave structure but which is not connected to the Newtonian solution branch. At fixed Weissenberg number, Wi and increasing Reynolds number from 3000-10000, this attractor goes from displaying a striation of weak polymer stretch localized at the critical layer to an extended sheet of very large polymer stretch. This transition can be attributed to a coil-stretch transition when the local Weissenberg number at the hyperbolic stagnation points of the Kelvin cat's eye structure of the TS wave exceed $1/2$. At $Re=10000$, unlike 3000, the Newtonian TS attractor evolves continuously into EIT as Wi is increased. We describe how the structure of the flow and stress fields changes, highlighting a "sheet-shedding" process by which the individual sheets associated with the critical layer structure break up to form the layered multisheet structure characteristic of EIT. We also find that at sufficiently high Wi , this solution family extends down in Reynolds number to between 150 and 200, indicating that viscoelasticity can sustain turbulence at Reynolds numbers well below Newtonian transition.

INTRODUCTION

Addition of long chain polymer molecules to a fluids has tremendous effects on wall-bounded turbulence, the most dramatic being the substantial reduction of the friction factor (Toms, 1949, 1977). This phenomenon has found wide use in applications that seek energy efficiency in flow processes. (Fink, 2012; Burger *et al.*, 1982; King, 2012).

This work describes recent results that have led to an improved understanding of this phenomenon. The main focus is channel flow of a dilute solution of high molecular weight polymer, so the ratio between solvent and total viscosity, β satisfies $1 - \beta \ll 1$, and the ratio between extensional and shear viscosities (Trouton ratio) Tr is $\gg 1$. For the FENE-P constitutive model with chain length parameter b , this requires that $b(1 - \beta) \gg 1$. This is the regime of primary relevance for drag reduction, where as a practical matter it is desired to keep the shear viscosity of the fluid low ($1 - \beta \ll 1$), but the extensional viscosity high ($b(1 - \beta) \gg 1$). The Reynolds number regime considered is $Re \sim 10^2 - 10^4$, i.e., near transition.

It is well-known that viscoelasticity suppresses the near-wall streamwise vortices that dominate Newtonian turbulence (Dubief *et al.*, 2004; Kim *et al.*, 2007; White & Mungal, 2008). A number of studies have captured this phenomena by studying the effect of viscoelasticity on three-dimensional (3D) nonlinear traveling wave solutions of the Navier-Stokes equations termed exact coherent states (ECS). (Stone *et al.*, 2002; Stone & Graham, 2003; Stone *et al.*, 2004; Li *et al.*, 2005, 2006; Li & Graham, 2007). These ECS contain the basic self-sustaining ingredients of transitional Newtonian turbulence i.e quasistreamwise vortices and streaks. A comprehensive review of ECS can be found in Graham & Floryan (2021).

Li and coworkers (Li *et al.*, 2006; Li & Graham, 2007) found that the ECS are so weakened by viscoelasticity that they

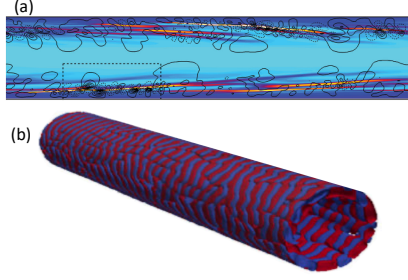


Figure 1. Snapshots of simulations of EIT in (a) channel flow (Terrapon *et al.*, 2014) and (b) pipe flow (Lopez *et al.*, 2019). In (a) color contours indicate polymer stretching and lines indicate vortex strength Q . In (a) isosurfaces indicate Q .

are no longer self-sustaining and lose existence. Recognizing that in general, viscoelasticity is not experimentally observed to drive relaminarization, these authors suggested the possibility of new viscoelastic mechanisms for turbulence coming into existence and being unmasked as the Newtonian structure are suppressed (Li *et al.*, 2006).

Indeed, instead of complete relaminarization (except in narrow parameter ranges at transitional Re), recent studies have unearthed a polymer-driven chaotic flow state dubbed elastoinertial turbulence (EIT) dominating the flow at high levels of viscoelasticity (Samanta *et al.*, 2013a). EIT (in this parameter regime) displays multilayered sheets of polymer stretch emanating from near the walls (see Figure 1a) and very weak, spanwise-oriented vortices – a sharp contrast to the 3D quasistreamwise vortex structures of Newtonian wall turbulence. Sid *et al.* (2018) have found that the sheetlike stress fluctuations that dominate simulations of EIT in channel flow are still present in 2D simulations, indicating that, in contrast with Newtonian turbulence, EIT is not fundamentally 3D. Similarly, near-wall localized, nearly-axisymmetric vortex and stress structures (Figure 1b) have been reported in pipe flow simulations of EIT (Lopez *et al.*, 2019). The present work aims to elucidate the origin of these structures.

FORMULATION

This study focuses on two-dimensional pressure-driven channel flow with constant mass flux. Two-dimensional flow is chosen because of the strongly spanwise-oriented structures observed in prior simulations in the EIT regime Sid *et al.* (2018). We also report some results from 3D simulations to indicate how these affect the main 2D structure. The x and y axes are aligned with the streamwise and wall-normal directions, respectively. Lengths are scaled by the half channel height l , so the dimensionless channel height $L_y = 2$. The domain is periodic in x with length L_x . Velocity v is scaled with the Newtonian laminar centerline velocity U ; time t with l/U , and pressure p with ρU^2 , where ρ is the fluid density. The polymer stress tensor τ_p is related to the polymer conformation tensor α through the FENE-P constitutive relation, which models each polymer molecule as a pair of beads connected by a nonlinear spring with maximum extensibility b .

We solve the momentum, continuity and FENE-P equa-

tions by direct numerical simulation (DNS):

$$\frac{\partial v}{\partial t} + v \cdot \nabla v = -\nabla p + \frac{\beta}{Re} \nabla^2 v + \frac{(1-\beta)}{ReWi} (\nabla \cdot \tau_p), \quad (1)$$

$$\nabla \cdot v = 0, \quad (2)$$

$$\tau_p = \frac{\alpha}{1 - \frac{\text{tr}(\alpha)}{b}} - I, \quad (3)$$

$$\frac{\partial \alpha}{\partial t} + v \cdot \nabla \alpha - \alpha \cdot \nabla v - (\alpha \cdot \nabla v)^T = \frac{-1}{Wi} \tau_p. \quad (4)$$

Here $Re = \rho U l / (\eta_s + \eta_p)$, where η_s and η_p are the solvent and polymer contributions to the zero-shear rate viscosity. The viscosity ratio $\beta = \eta_s / (\eta_s + \eta_p)$. We fix $\beta = 0.97$ and $b = 6400$. Since $1 - \beta$ is proportional to polymer concentration and b to the number of monomer units, these parameters correspond to a dilute solution of a high molecular weight polymer. The Weissenberg number $Wi = \lambda U / l$, where λ is the polymer relaxation time.

For integrating the momentum equation, second-order central differences were used for spatial discretization, and second-order Adams-Bashforth and Crank-Nicholson methods were used for time-integration of the convection and diffusion terms, respectively. The FENE-P equation was discretized using a high resolution central difference scheme.

Using computations in channel flow at $Re = 1500$, Shekar *et al.* (2019) observed a narrow zone of Wi where the only attractor was the laminar base state. This zone separated drag-reduced Newtonian turbulence at lower Wi and EIT at higher Wi , corroborating the experimental observations of Choueiri *et al.* (2018). The laminar flow remains linearly stable in the EIT regime, but only very small (but finite) perturbations are sufficient to drive the flow to EIT. EIT in this parameter regime displays polymer stretch fluctuations localized near the wall. In particular, a clear resemblance was noted between the EIT structure and the viscoelastic extension of the classical Tollmien-Schlichting (TS) mode, which at the chosen parameters is the slowest decaying mode from linear stability analysis. Similarly, resolvent analysis predicts strong amplification of this structure in the presence of viscoelasticity. This strong amplification implies, consistent with the fully nonlinear results, that even very weak disturbances may be sufficient to trigger EIT.

The viscoelastic TS mode displays polymer stretch fluctuations that are sharply localized to critical layers, i.e wall-normal positions near the top and bottom walls where the streamwise velocity equals the real part of the wave speed. Critical layers can be thought of as the most favorable positions for energy exchange between the mean and fluctuations, because they are the positions where both have the same speed. These results indicate a role for TS-like critical layer mechanisms at EIT.

The key observations from Shekar *et al.* (2019) are summarized in Figure 2. Fig. 2a shows a snapshot from the 3D DNS, illustrating the sharp localization of stretch fluctuations in a layer near the wall. Except in the layers where the stress fluctuations are largest, this flow is dominated by structures with a wavelength of half the domain size (i.e. 5 channel half-heights). Fig. 2b shows the structure filtered to keep only this wavelength. Fig. 2c shows the slowest decaying structure from linear stability analysis at a wavelength of 5 – this is the viscoelastic continuation of the linear Tollmien-Schlichting mode. Finally, Fig. 2d shows the most amplified resolvent mode under the same conditions. The resemblance of the full nonlinear structure to the TS mode is apparent.

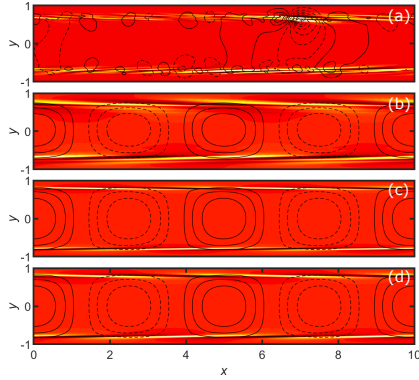


Figure 2. Summary of results at $Re = 1500$ (Shekar *et al.*, 2019). (a) Snapshot of v' (line contours) and α'_{xx} (filled contours) from 3D nonlinear DNS at $Re = 1500$, $Wi = 20$, where $'$ denotes fluctuations. (b) Phase-matched average $(k_x L_x / 2\pi, k_z L_z / 2\pi) = (2, 0)$ structures from 3D DNS. (c) Structure of the TS mode at $Re = 1500$, $Wi = 20$, and the same wavenumbers as in (b). (d) Structure of the most strongly amplified resolvent mode at $Re = 1500$, $Wi = 20$, the same wavenumbers as in (b), and $c = 0.37$. In all plots, contour levels are symmetric about zero. For v' dashed - negative, solid - positive. For α'_{xx} black - negative, red - zero and yellow - positive.

Building on the above observations, we turn to elucidating the role of Tollmien-Schlichting wave structures in EIT. In contrast to $Re = 1500$, at $Re = 3000$ a nonlinear self-sustaining TS wave exists in the Newtonian limit. For $Wi \gtrsim 6$, we find a viscoelastic family of attractors whose structure is virtually identical to the linear TS mode, and in particular exhibits strongly localized stress fluctuations at the critical layer position of the TS mode. A snapshot of one of these solutions, at $Wi = 10$, $L_x = 5$, is shown in Figure 3; note the close resemblance to Figure 2c. At the parameter values chosen, this solution branch is not connected to the nonlinear TS solution branch found for Newtonian flow, and thus represents a solution family that is nonlinearly self-sustained by viscoelasticity (Shekar *et al.*, 2020). (The laminar state remains linearly stable, though again, as in Shekar *et al.* (2019), only an extremely small perturbation is required to drive the solution away from laminar.) Evidence indicates that this branch is connected through an unstable solution branch to two-dimensional elastoinertial turbulence (EIT).

Now moving up from $Re = 3000$ to $Re = 10000$, it is found that *the Newtonian nonlinear TS wave solutions attractor evolves continuously and without hysteresis into EIT as Wi is increased from zero to about 13 – the two flows are part of the same solution family* (Shekar *et al.*, 2021). The snapshots in Figure 4 illustrate the evolution of the flow and stress fields as Wi increases. Figure 4a shows the self-sustained nonlinear Tollmien-Schlichting wave in the Newtonian limit $Wi = 0$. As Wi increases to 4, sheets of polymer stretch appear, driven by the extensional flow at the hyperbolic stagnation points of the Kelvin cat's eye structure of the TS wave. As Wi increases further, the simple sheet structures that originate with the TS critical layer structure evolve into the multilayered structure of EIT through a process that we call “sheet-shedding”: Individual sheets associated with the critical layer structure break up, with the fragments further sheared as they travel downstream. An intermediate stage of this process ($Wi = 8$) is shown in Figure 4c. Finally as Wi increases further, the typical overlapping sheet structure becomes fully developed, as illustrated in

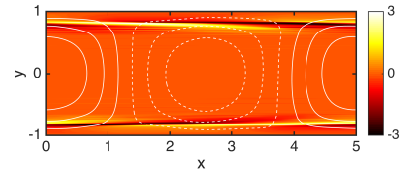


Figure 3. (a) Snapshot of the finite amplitude Tollmien-Schlichting wave solution at $Re = 3000$, $Wi = 10$. White contours are wall-normal velocity, colors are deviations of xx polymer stretch from laminar.

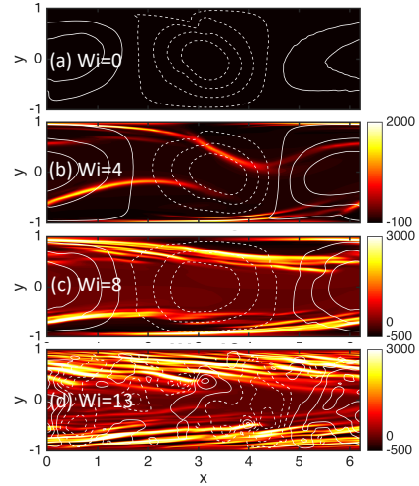


Figure 4. Snapshots of the finite amplitude Tollmien-Schlichting wave solution at $Re = 10000$ and (a) $Wi = 0$, (b) $Wi = 4$, (c) $Wi = 8$, (d) $Wi = 13$. White contours are wall-normal velocity, colors are deviations of xx polymer stretch from laminar.

Figure 4d. Note the resemblance between this structure and Figure 1a.

An important question is the robustness of two dimensional result to three-dimensional perturbations. In particular, given the tilted-sheet structure of the stress fluctuations, one might expect that a 3D perturbation that changes the position of these sheets will expose different parts of the sheet to different streamwise velocities – a portion of the sheet perturbed toward the centerplane will be convected faster than a portion perturbed toward the wall. This velocity differential might be expected to tend to tear the sheets apart. Figure 5a-b show snapshots of α_{xx} at $y = 0.8$ at two instants from a 3D simulation at $Re = 2000$, $Wi = 30$ that starts from a 2D initial condition subjected to small random perturbations. Since the sheets are tilted with respect to the flow direction, this view “slices” obliquely through the sheets of stress. At short time ($t = 36$, Fig. 5a), the sheets are coherent in the z direction, but as time proceeds, ($t = 180$, Fig. 5), they become less so. Figure 5c shows a 3d view of the structure at $t = 180$, illustrating how the sheets are perturbed in 3D. As the sheets lose coherence, the overall structure becomes weaker and the drag closer to the laminar value. Nevertheless the basic sheet structure remains.

We began this discussion with results at $Re = 1500$, well below the regime where the Newtonian flow becomes linearly unstable and also below the limiting Reynolds number for the existence of self-sustaining nonlinear Tollmien-Schlichting waves in that limit. The existence of nontrivial flows at finite Wi in these cases illustrates the strongly subcritical nature of the origin of these structures. Many studies (e.g. Samanta *et al.*

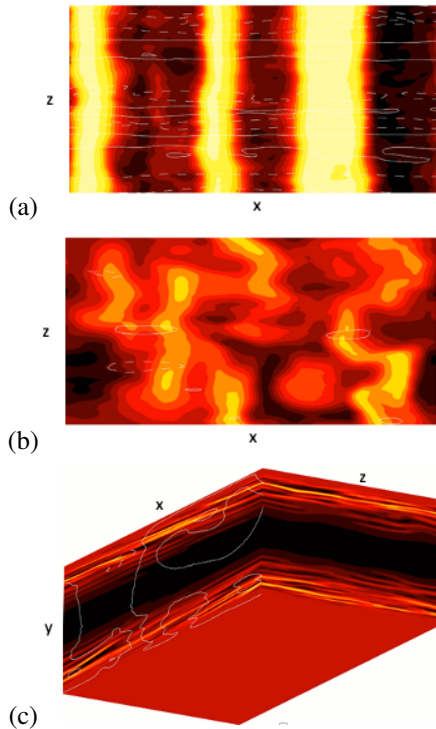


Figure 5. Snapshots illustrating evolution of 3d α_{xx} structure from 2d EIT at $Re = 2000, Wi = 30, L_x = 6.2, L_z = 3.1$. Flow is left to right. (a) Slice at $y = 0.8, t = 36$. (b) As in (a) but at $t = 180$. (c) 3D view showing side, front and bottom.

(2013a)) have indicated that turbulence in viscoelastic flows can exist at Reynolds numbers well below the Newtonian onset value, so we conclude this study by examining the solution family we have found as Re decreases below the regime considered above.

To do this, we have done DNS at $Wi = 30$, starting at $Re = 10000$ and incrementally decreasing Re , letting the solution reach statistical steady state before further decreasing Re . At $Wi = 30$, the viscoelastic TS wave (EIT) solution family persists down to Re between 150 and 200. Figure 6 shows the time-averaged norm of α_{xx} fluctuations vs. Re . Figure 7 shows a snapshot of the stress structure at $Re = 400$, revealing that the near-wall sheetlike structure persists. Preliminary results indicate that as Wi increases to 50, a very similar threshold Reynolds number is found. These results may be connected to observations of non-laminar flow in polymer solutions at Reynolds numbers below transition (Samanta *et al.*, 2013b). A number of other recent works have also examined the issue of turbulent (or at least non-laminar) flow in rectilinear viscoelastic flows at low Reynolds number Buza *et al.* (2022a,b) Khalid *et al.* (2021). Those studies indicate the presence of viscoelastic instability and nonlinear self-sustaining structures even at vanishingly small Re , with a stress structure that is localized near the centerplane, rather than near the walls as we observe here. Therefore, multiple structures and mechanisms seem to exist for emergence of nonlaminar flows of viscoelastic fluids even at low Re . Experimental observations in pipe flow (Choueiri *et al.*, 2021) are consistent the emergence of “center mode” fluctuations at low Re , which evolve toward “wall-modes” as Re increases.

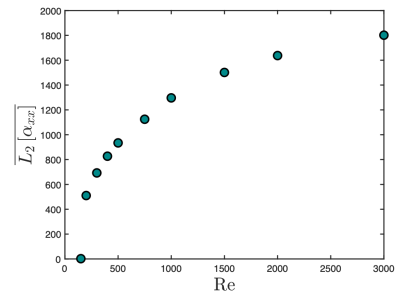


Figure 6. Norm of stress fluctuations vs. Re at $Wi = 30$.

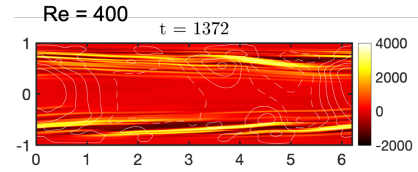


Figure 7. Snapshot of EIT solution at $Re = 400, Wi = 30$. White contours are wall-normal velocity, colors are deviations of xx polymer stretch from laminar.

REFERENCES

- Burger, E.D., Munk, W.R. & Wahl, H.A. 1982 Flow increase in the trans Alaska pipeline through use of a polymeric drag-reducing additive. *Journal Of Petroleum Technology* **34** (2), 377–386.
- Buza, Gergely, Beneitez, Miguel, Page, Jacob & Kerswell, Rich R 2022a Finite-amplitude elastic waves in viscoelastic channel flow from large to zero Reynolds number. *arXiv*.
- Buza, Gergely, Page, Jacob & Kerswell, Rich R. 2022b Weakly nonlinear analysis of the viscoelastic instability in channel flow for finite and vanishing Reynolds numbers. *Journal of Fluid Mechanics* **940**, A11.
- Choueiri, George H, Lopez, Jose M & Hof, Björn 2018 Exceeding the Asymptotic Limit of Polymer Drag Reduction. *Phys. Rev. Lett.* **120** (12), 124501.
- Choueiri, George H., Lopez, Jose M., Varshney, Atul, Sankar, Sarath & Hof, Björn 2021 Experimental observation of the origin and structure of elastoinertial turbulence. *Proceedings of the National Academy of Sciences* **118** (45), e2102350118.
- Dubief, Yves, White, Christopher M, Terrapon, Vincent E, Shaqfeh, Eric S G, Moin, Parviz & Lele, Sanjiva K 2004 On the coherent drag-reducing and turbulence-enhancing behaviour of polymers in wall flows. *J. Fluid Mech.* **514**, 271–280.
- Fink, Johannes Karl 2012 *Petroleum Engineer’s Guide to Oil Field Chemicals and Fluids*. Gulf Professional Publishing.
- Graham, Michael D & Floryan, Daniel 2021 Exact Coherent States and the Nonlinear Dynamics of Wall-Bounded Turbulent Flows. *Annu Rev Fluid Mech* **53**, 227–253.
- Khalid, Mohammad, Shankar, V. & Subramanian, Ganesh 2021 Continuous Pathway between the Elasto-Inertial and Elastic Turbulent States in Viscoelastic Channel Flow. *Physical Review Letters* **127** (13), 134502.
- Kim, Kyoungyoun, Li, Chang-F, Sureshkumar, R, Balachandrar, S & Adrian, Ronald J 2007 Effects of polymer stresses on eddy structures in drag-reduced turbulent channel flow. *J. Fluid Mech.* **584**, 281–299.
- King, George Everette 2012 Hydraulic Fracturing 101: What Every Representative, Environmentalist, Regulator, Re-

- porter, Investor, University Researcher, Neighbor and Engineer Should Know About Estimating Frac Risk and Improving Frac Performance in Unconventional Gas and Oil Wells. In *SPE Hydraulic Fracturing Technology Conference*. The Woodlands, TX: Society of Petroleum Engineers.
- Li, Wei & Graham, Michael D 2007 Polymer induced drag reduction in exact coherent structures of plane Poiseuille flow. *Phys. Fluids* **19** (8), 083101.
- Li, W, Stone, P A & Graham, Michael D 2005 Viscoelastic nonlinear traveling waves and drag reduction in plane Poiseuille flow. *Fluid Mechanics and its Applications: Proceedings of the IUTAM Symposium on Laminar-Turbulent Transition and Finite Amplitude Solutions* **77**, 285–308.
- Li, Wei, Xi, Li & Graham, Michael D 2006 Nonlinear traveling waves as a framework for understanding turbulent drag reduction. *J. Fluid Mech.* **565**, 353–362.
- Lopez, Jose M, Choueiri, George H & Hof, Björn 2019 Dynamics of viscoelastic pipe flow at low Reynolds numbers in the maximum drag reduction limit. *J. Fluid Mech.* **874**, 699–719.
- Samanta, Devranjan, Dubief, Yves, Holzner, Markus, Schäfer, Christof, Morozov, Alexander N, Wagner, Christian & Hof, Björn 2013a Elasto-inertial turbulence. *Proc. Nat. Acad. Sci.* **110** (26), 10557–10562.
- Samanta, Devranjan, Dubief, Yves, Holzner, Markus, Schäfer, Christof, Morozov, Alexander N, Wagner, Christian & Hof, Björn 2013b Elasto-inertial turbulence. *Proceedings of the National Academy of Sciences* **110** (26), 10557–10562.
- Shekar, Ashwin, McMullen, Ryan M., McKeon, Beverley J. & Graham, Michael D. 2020 Self-sustained elastoinertial Tollmien–Schlichting waves. *Journal of Fluid Mechanics* **897**, A3.
- Shekar, Ashwin, McMullen, Ryan M., McKeon, Beverley J. & Graham, Michael D. 2021 Tollmien–Schlichting route to elastoinertial turbulence in channel flow. *Physical Review Fluids* **6**, 093301.
- Shekar, Ashwin, McMullen, Ryan M, Wang, Sung-Ning, McKeon, Beverley J & Graham, Michael D 2019 Critical-Layer Structures and Mechanisms in Elastoinertial Turbulence. *Phys. Rev. Lett.* **122** (12), 124503.
- Sid, S, Terrapon, V E & Dubief, Y 2018 Two-dimensional dynamics of elasto-inertial turbulence and its role in polymer drag reduction. *Phys. Rev. Fluids* **3** (1), 011301.
- Stone, PA & Graham, Michael D 2003 Polymer dynamics in a model of the turbulent buffer layer. *Phys. Fluids* **15** (5), 1247–1256.
- Stone, PA, Waleffe, F & Graham, Michael D 2002 Toward a structural understanding of turbulent drag reduction: Non-linear coherent states in viscoelastic shear flows. *Phys. Rev. Lett.* **89** (20), 208301.
- Stone, Philip A, Roy, Anshuman, Larson, Ronald G, Waleffe, Fabian & Graham, Michael D 2004 Polymer drag reduction in exact coherent structures of plane shear flow. *Phys. Fluids* **16** (9), 3470–3482.
- Terrapon, Vincent E, Dubief, Yves & Soria, Julio 2014 On the role of pressure in elasto-inertial turbulence. *J Turbul* **16** (1), 26–43.
- Toms, B. A. 1949 In *Proc. Int. Congr. Rheology*. North-Holland.
- Toms, B. A. 1977 On the early experiments on drag reduction by polymers. *Phys. Fluids* **20**, S3–S8.
- White, Christopher M & Mungal, M Godfrey 2008 Mechanics and prediction of turbulent drag reduction with polymer additives. *Annu Rev Fluid Mech* **40**, 235–256.